Photoemission spectroscopy study of metal-insulator transition in $SrMn_{1-x}Fe_xO_3$

D. H. Kim,[1] H. J. Lee,[1] B. Dabrowski,[2] S. Kolesnik,[2] Jieun Lee,[3] Bongjae Kim,[3] B. I. Min,[3] and J.-S. Kang[1,*]
[1]*Department of Physics, The Catholic University of Korea (CUK), Bucheon 420-743, Korea*
[2]*Department of Physics, Northern Illinois University, DeKalb, Illinois 600115, USA*
[3]*Department of Physics, POSTECH, Pohang 790-784, Korea*
(Received 30 August 2009; revised manuscript received 30 December 2009; published 1 February 2010)

Electronic structures of cubic perovskite oxides of $SrMn_{1-x}Fe_xO_3(0 \leq x \leq 1)$ have been investigated by employing photoemission spectroscopy (PES) and soft x-ray absorption spectroscopy (XAS). The spectral intensity near the Fermi level $[I(E_F)]$ is found to be finite in Fe $3d$ PES of $SrFeO_3$. $I(E_F)$ increases with x in Fe $3d$ PES of $SrMn_{1-x}Fe_xO_3$, while it is negligibly small in Mn $3d$ PES for all x. The O $1s$ XAS for $SrFeO_3$ also shows the finite spectral intensity near the Fermi level. These findings provide the experimental evidence for the metal-insulator transition in $SrMn_{1-x}Fe_xO_3$ with decreasing x and imply the importance of Fe $3d$ electrons in determining the metallic states in $SrMn_{1-x}Fe_xO_3$. First principles band structure calculations for $SrFeO_3$ and $SrMnO_3$ support these findings in PES/XAS.

DOI: 10.1103/PhysRevB.81.073101 PACS number(s): 79.60.−i, 74.25.Jb, 78.70.Dm, 71.30.+h

Since the discovery of colossal magnetoresistance (CMR) phenomenon in perovskite manganites, the ferromagnetic interaction between transition-metal (T) ions and the metal-insulator transition (MIT) in perovskite oxides have attracted much attention. In this aspect, perovskite cubic oxides of $SrMn_{1-x}Fe_xO_3$ are very interesting, because $Fe^{4+}(3d^4)$ ion is isoelectronic with $Mn^{3+}(3d^4)$ ion. $SrMn_{1-x}Fe_xO_3$ with $Mn^{4+}(t_{2g}^3)$ and $Fe^{4+}(t_{2g}^3e_g^1)$ ions is expected to demonstrate the competing spin, charge, and lattice interactions. In contrast to perovskite manganites, however, $SrFeO_3$ shows the metallic behavior when fully oxygenated.[1–3] Furthermore, $SrFeO_3$ exhibits neither the Jahn-Teller (JT) distortion[3,4] nor the orbital ordering,[5] which is unusual considering that high-spin (HS) $Fe^{4+}(t_{2g}^3e_g^1)$ ions are usually JT active. The metal-insulator transition (MIT) is observed in $SrFeO_{3-\delta}$,[3] which is likely to be accompanied by the charge ordering (CO) of mixed-valent Fe^{3+}/Fe^{4+} ions. With the Mn substitution in $SrFeO_3$, the system becomes an insulator. Both $SrMnO_3$ and $SrFeO_3$ show the antiferromagnetic (AF) ordering with the Neel temperatures of $T_N=233$ K for $SrMnO_3$ (the G type[6]) and $T_N=134$ K for $SrFeO_3$ (the spiral type).[7] At an intermediate substitution, cubic $SrMn_{1-x}Fe_xO_3$ shows rapid suppression of both the G- and spiral-type AF ordering and exhibits the AF ordering and/or the spin-glass behavior.[5]

Mössbauer measurements[5,8] for $SrMn_{1-x}Fe_xO_3$ revealed that there are two types of Fe ions for $x<1$, which were considered to be in the charge disproportionation (CD) of $Fe^{3+}(d^5)+Fe^{5+}(d^3)$. On the other hand, the analysis of x-ray photoemission spectra for isoelectronic $CaFeO_3$ suggested that the CO state results from the CD of ligand holes $[2(d^5\underline{L}) \rightarrow d^5\underline{L}^2+d^5]$ rather than the CD of Fe-d electrons $[2d^4 \rightarrow d^3+d^5]$ ($\underline{L}$: an oxygen hole, or a ligand hole).[9–11] However, in our recent work based on soft x-ray absorption spectroscopy (XAS),[12] we have shown that both Fe and Mn ions are formally tetravalent (Mn^{4+}, Fe^{4+}) in $SrMn_{1-x}Fe_xO_3$. Hence the valence states of Fe and Mn ions in $SrMn_{1-x}Fe_xO_3$ have been controversial.

In this work, we have investigated the correlation between the electronic structures of $SrMn_{1-x}Fe_xO_3$ and the MIT by using soft x-ray photoemission spectroscopy (PES) and soft x-ray absorption spectroscopy (XAS). These methods are powerful experimental tools for studying the electronic structures of solids. Then we have compared the experimental data with the *ab initio* band structure calculations.

Polycrystalline samples of stoichiometric $SrMn_{1-x}Fe_xO_3$ $(0 \leq x \leq 1)$ were prepared by using a two-step synthesis methods, as described in Ref. 5. PES experiment was performed at the 2A undulator beamline of Pohang light source (PLS). Samples were cleaned *in situ* by repeated scraping with a diamond file under the base pressure of $\sim 5 \times 10^{-11}$ Torr. PES spectra were obtained at room temperature by using a SCIENTA SES100 analyzer. The Fermi level E_F and the overall energy resolution of the system [FWHM: full width at half maximum] were determined from the Fermi-edge spectrum of scraped Au metal in electrical contact with samples. The FWHM of the valence-band PES spectra was set at ~150 meV at $h\nu \sim 600$ eV. PES spectra were normalized to the incident photon flux.

Figure 1(a) shows the valence-band PES spectra of $SrMnO_3$, obtained by employing Mn $2p \rightarrow 3d$ resonant photoemission spectroscopy (RPES). The marks from A-F represent the $h\nu$ values, where Mn $2p \rightarrow 3d$ RPES spectra were obtained: A: $h\nu=637$ eV, B: $h\nu=640$ eV, C: $h\nu \approx 641$ eV, D: $h\nu=642$ eV, E: $h\nu=643$ eV, F: $h\nu=646$ eV. The inset of Fig. 1 shows the Mn $2p_{3/2}$ XAS of $SrMnO_3$. This Mn $2p_{3/2}$ XAS reveals that Mn ions are formally tetravalent $(3d^3)$ in $SrMnO_3$, which was confirmed in our previous work.[12] It is well known that the $3d$ electron emissions of T ions are enhanced in T $2p \rightarrow 3d$ RPES (Ref. 13) and that T $2p \rightarrow 3d$ RPES has the advantage of being more *bulk* representative than T $3p \rightarrow 3d$ RPES that occurs at lower $h\nu$'s.

It is clearly observed that the feature around ~2 eV binding energy (BE) is strongly enhanced in Mn $2p \rightarrow 3d$ RPES, indicating that this peak has the large Mn $3d$ character. The second feature at ~6 eV BE is due to the O $2p$ states that are hybridized to the Mn $3d$ states [see also Fig. 1(b)]. The broad features at higher BE's, which shift away from E_F with increasing $h\nu$ (marked with bars), are the Mn Auger peaks since they appear at constant kinetic energies. These Auger emissions are also enhanced at the Mn $2p$ absorption edge, as observed in other manganese oxides.[13] Similarly as in

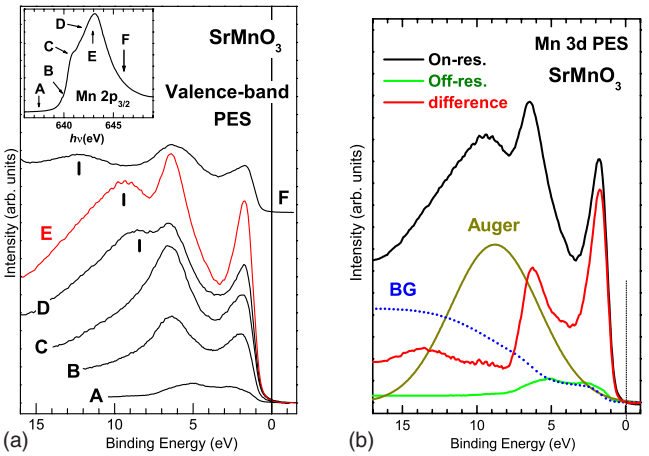

FIG. 1. (Color online) (a) Valence-band PES spectra of $SrMnO_3$ near the Mn $2p \rightarrow 3d$ absorption edge. The Fermi level E_F corresponds to 0 eV in binding energy. The labels of A–F correspond to the $h\nu$'s, marked in the inset. Inset: Mn $2p_{3/2}(L_3)$ XAS of $SrMnO_3$. (b) Extraction procedures for Mn $3d$ PES. See the text for the details.

$SrMnO_3$, Fe $2p \rightarrow 3d$ RPES also exhibits the resonant enhancement of Fe $3d$ electron emission for $x > 0$ in $SrMn_{1-x}Fe_xO_3$. The Fe $3d$ resonance occurs around $\sim 2-3$ eV BE, indicating that it has the large Fe $3d$ character. The raw RPES data are not shown in this paper, but such features are recognized in Fig. 2.

Figure 1(b) shows the procedure to extract the contributions from the Mn $3d$ PES in the valence-band PES spectrum of $SrMnO_3$. Black and green curves correspond to the on-resonance and off-resonance spectra, respectively. The curve, labeled as "Auger," denotes the contributions of the Mn *LMM* Auger peak, which was explained in Fig. 1(a). The dotted line, labeled as "BG," represents the rough estimation of the inelastic background. Then the difference curve (red), obtained by subtracting the off-resonance spectrum, the *LMM* Auger spectrum, and the inelastic BG from the on-resonance spectrum, represents roughly the partial spectral weight distribution of the Mn $3d$ electrons.[13] So we consider this difference as Mn $3d$ PES of $SrMnO_3$.

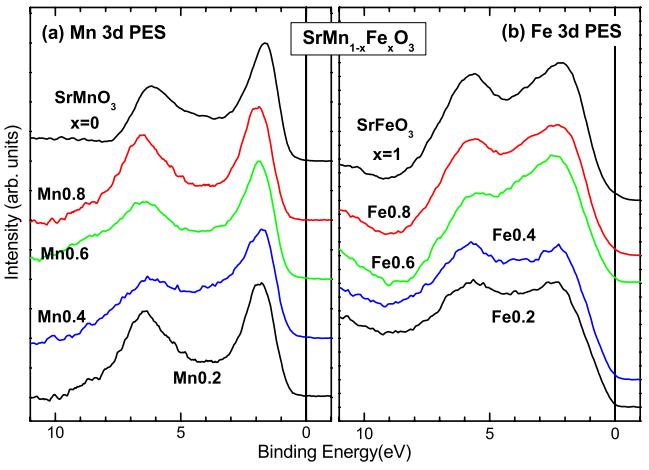

FIG. 2. (Color online) (a) Comparison of the extracted Mn $3d$ PES and (b) the extracted Fe $3d$ PES of $SrMn_{1-x}Fe_xO_3$.

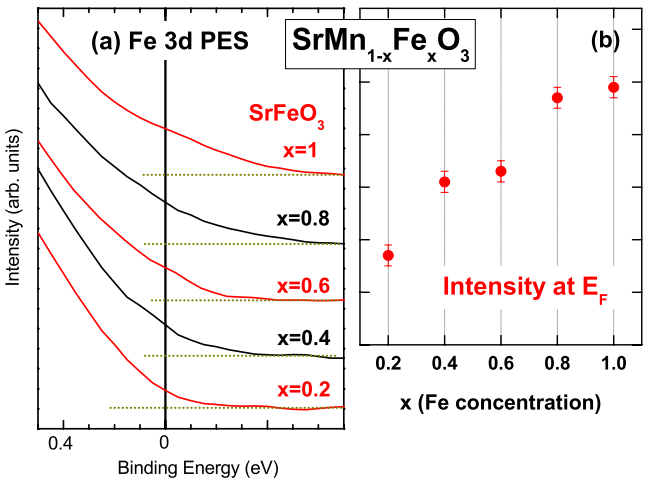

FIG. 3. (Color online) (a) The enlarged comparison of the extracted Fe $3d$ PES of $SrMn_{1-x}Fe_xO_3$. These Fe $3d$ PES data are scaled at the main peak around ~ 2 eV binding energy. (b) Plot of the intensity of the Fe $3d$ PES near E_F versus x in $SrMn_{1-x}Fe_xO_3$. Error bars are denoted in this figure.

Figures 2(a) and 2(b) show the extracted Mn $3d$ PES and Fe $3d$ PES of $SrMn_{1-x}Fe_xO_3 (0 \leq x \leq 1)$, respectively. Each $3d$ PES spectrum has been determined following the extraction procedure, which was described in Fig. 1(b). It is found that, as x varies, the large-energy-scale features of the extracted Mn $3d$ PES and Fe $3d$ PES are more or less unchanged in $SrMn_{1-x}Fe_xO_3$. Both the Mn $3d$ PES in $SrMnO_3$ and Fe $3d$ PES in $SrFeO_3$ exhibit a double-peak structures, one around ~ 2 eV BE and another around ~ 6 eV BE. All the Mn $3d$ PES spectra of $SrMn_{1-x}Fe_xO_3$ exhibit a sharp peak ~ 2 eV below E_F, which is attributed to the occupied Mn $t_{2g}^3\uparrow$ states for $Mn^{4+}(3d^3)$ ions[12] ($\uparrow$ denotes the majority spin). Fe $3d$ PES spectra exhibit a rather broad peak centered around ~ 2 eV BE and the weak emission near E_F, which are identified as the occupied Fe $t_{2g}^3\uparrow$ states and $e_g^1\uparrow$ states, respectively, since Fe ions are tetravalent $(3d^4)$ in $SrMn_{1-x}Fe_xO_3$.[12] The broad feature around 6–7 eV in BE in both Mn $3d$ and Fe $3d$ PES are the O $2p$-Mn/Fe $3d$ hybridized states. The large O $2p$ electron character in Mn/Fe $3d$ PES spectra suggests the strong hybridization between Mn/Fe $3d$ and O $2p$ states in $SrMn_{1-x}Fe_xO_3$.

The main difference between Mn $3d$ PES and Fe $3d$ PES is that the spectral weight near $E_F[I(E_F)]$ is finite in Fe $3d$ PES, while $I(E_F)$ is negligible in Mn $3d$ PES. Indeed $I(E_F)$ in Fe $3d$ PES increases with increasing x (x: the concentration of Fe ions). This trend is shown more clearly in Fig. 3, which shows the enlarged comparison of the extracted Fe $3d$ PES and plots $I(E_F)$ versus x in $SrMn_{1-x}Fe_xO_3$. This finding agrees well with the MIT in $SrMn_{1-x}Fe_xO_3$ with decreasing x,[5] and implies that Fe $3d$ electrons play an important role in determining the metallic conductivity in $SrMn_{1-x}Fe_xO_3$. Further, the broader PES peak in Fe $3d$ PES than in Mn $3d$ PES reflects the larger bandwidth of Fe $3d$ bands than that of Mn $3d$ bands. In other words, Fe $3d$ electrons are more itinerant than Mn $3d$ electrons, which is due to the stronger Fe $3d$-O $2p$ hybridization than the Mn $3d$-O $2p$ hybridization. The large Fe $3d$-O $2p$ covalency is consistent with the

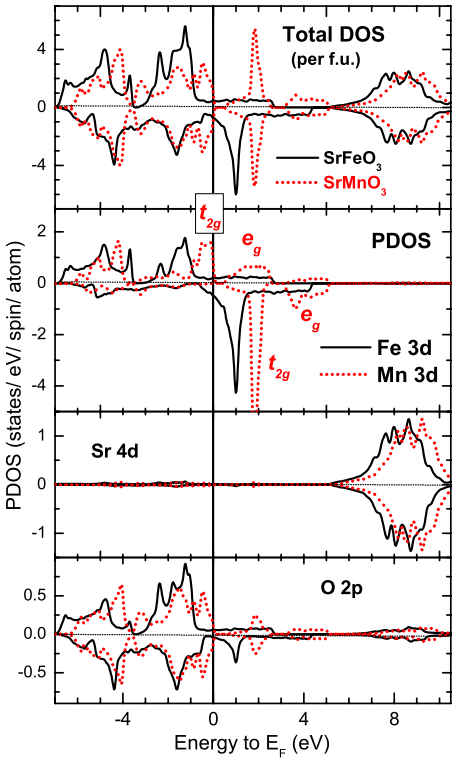

FIG. 4. (Color online) Comparison of the calculated DOS's of $SrFeO_3$ (black solid lines) and $SrMnO_3$ (red dotted lines). From Top to bottom are shown the total DOS, the Fe/Mn 3*d* PDOS, the Sr 4*d* PDOS, and the O 2*p* PDOS. Except for the total DOS, which is shown in the units of (states/eV/spin/f.u.), all the PDOS's are shown in the units of (states/eV/spin/atom).

absence of the JT distortion in $SrFeO_3$. This conclusion is also consistent with the experimental signature of the increasing covalency of the Fe-O bond for larger x in $SrMn_{1-x}Fe_xO_3$, which was concluded from XRD measurements.[5]

The origin of the increasing $I(E_F)$ with increasing x in $SrMn_{1-x}Fe_xO_3$ needs to be clarified. It probably has something to do with the polaron formation due to the JT active Fe^{4+} ion. Even though $SrFeO_3$ does not exhibit the JT distortion, there will be the dynamical JT phonons that couple with electron carriers. Then the JT polarons, which are less mobile than bare carriers, are formed so as to suppress $I(E_F)$ (see Fig. 5).[14] For small x, the polaron hopping hardly occurs, and $I(E_F)$ would be very weak. With increasing x, the polaron hopping occurs increasingly, and so $I(E_F)$ will be enhanced. In this way, one can qualitatively understand the increase of $I(E_F)$ in the Fe 3*d* PES based on the polaron formation due to the dynamical JT effect in $SrMn_{1-x}Fe_xO_3$.

Figure 4 shows the calculated total densities of states (DOS's) and partial densities of states (PDOS's) of $SrFeO_3$ and $SrMnO_3$. These were obtained by using the self-consistent full-potential linearized augmented plane wave (FLAPW) band method[15] within the generalized gradient approximation (GGA).[16] In these calculations, the ferromagnetic ground state[17] was assumed for $SrFeO_3$ and the *G*-type antiferromagnetic ground state was assumed for $SrMnO_3$. These band structure calculations produce the correct insulating ground state for $SrMnO_3$ and the metallic ground state for $SrFeO_3$. The calculated Mn 3*d* states show a gap between the occupied $t_{2g}\uparrow$ states and the unoccupied $t_{2g}\downarrow$ and $e_g\uparrow\downarrow$ states (see the second panel). In $SrFeO_3$, the Fermi level lies in the Fe $e_g\uparrow$ states, and thus the $t_{2g}\uparrow$ bands are fully occupied, the $e_g\uparrow$ bands are partially occupied, and the $t_{2g}\downarrow$ and $e_g\downarrow$ bands are unoccupied. Note that the unoccupied Fe $t_{2g}\downarrow$ bands are located closer to E_F than the unoccupied Mn $e_g\uparrow$ and $t_{2g}\downarrow$ bands, and the metallic Fermi edge lies in the partially occupied Fe $e_g\uparrow$ states. Such trends in the peak positions are consistent with the measured PES/XAS spectra (see Fig. 5). The main contributions near E_F come from the Fe/Mn 3*d* states. The Sr 4*d* states are located far above E_F and do not contribute to the states near E_F. The unoccupied Sr 4*d* states in $SrFeO_3$ are located closer to E_F than those in $SrMnO_3$. This trend agrees with that in the measured O 1*s* XAS spectra.[12] The O 2*p* states exhibit a large hybridization with Fe/Mn 3*d* states, and the states between ~−4 and ~−8 eV are mainly due to the O 2*p* bands.

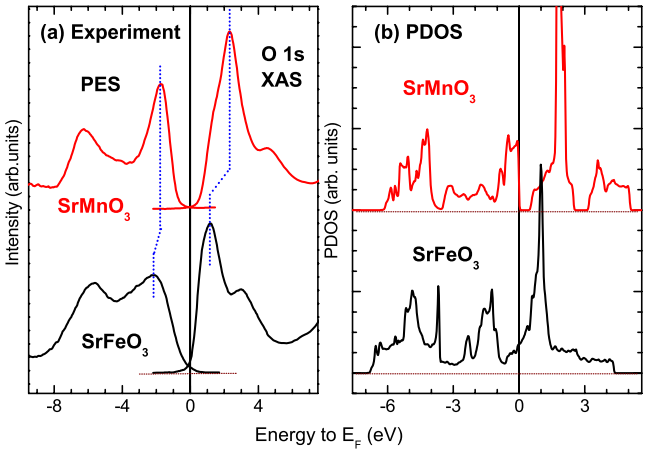

FIG. 5. (Color online) (a) Left: the extracted Mn 3*d* and Fe 3*d* PES for $SrMnO_3$ and $SrFeO_3$, respectively. (Right) The O 1*s* XAS spectra of $SrMnO_3$ and $SrFeO_3$. (b) Calculated Mn 3*d* PDOS for $SrMnO_3$ and Fe 3*d* PDOS for $SrFeO_3$.

Figure 5(a) shows the combined Mn and Fe 3*d* PES spectra and the O 1*s* XAS spectra[18] of $SrMnO_3(x=0)$ and $SrFeO_3(x=1)$, respectively. The O 1*s* XAS spectrum[12] can be considered to represent the unoccupied *T* 3*d*, *T sp*, and Sr 4*d* states via the hybridization with the O 2*p* states. The lowest-energy peaks in the O 1*s* XAS of $SrMnO_3$ and $SrFeO_3$ correspond to the overlapping unoccupied Mn/Fe 3*d* $e_g\uparrow$ and $t_{2g}\downarrow$ states, and the shoulders at the higher energy side correspond to the unoccupied Mn/Fe 3*d* $e_g\downarrow$ states. Note that both Fe 3*d* PES and O 1*s* XAS for $SrFeO_3$ exhibit the finite spectral weight near E_F, while those for $SrMnO_3$ exhibit the negligible spectral weight near E_F. This difference provides experimental evidence for the metallic ground state of $SrFeO_3$ and the insulating ground state of $SrMnO_3$. In the O 1*s* XAS, the lowest-energy peak in $SrFeO_3$ lies closer to E_F than that in $SrMnO_3$, which agrees with the trend in the calculated PDOS in Fig. 4(b).

Figure 5(b) shows the calculated PDOS for Mn 3*d* states of $SrMnO_3$ and for Fe 3*d* states of $SrFeO_3$. The features of the gap in $SrMnO_3$ and the metallic PDOS in $SrFeO_3$ agree

with experiment. Further, the trend in the calculated peak positions agrees well with that in PES/XAS, suggesting that the calculated GGA electronic structures for $SrMnO_3$ and $SrFeO_3$ support the major findings of the PES/XAS experiment. On the other hand, the absolute peak positions in the calculated PDOS's are somewhat different from those in PES/XAS. But such discrepancies are often found in the GGA band structure calculations, when the on-site Coulomb correlation interaction of T $3d$ electrons is neglected.[19,20] Thus the small differences in peak positions between theory and experiment indicate the non-negligible Coulomb correlation in Fe/Mn $3d$ electrons in $SrMn_{1-x}Fe_xO_3$.

In conclusion, the valence-band PES study for $SrMn_{1-x}Fe_xO_3$ shows that the occupied Mn $3d$ states with the $t_{2g}^3\uparrow$ (Mn^{4+}) configuration are located about ~ 2 eV below E_F and that the Fe $3d$ PES due to the Fe^{4+} ions ($t_{2g}^3\uparrow e_g^1\uparrow$) are broader than the Mn $3d$ PES. The finite $I(E_F)$ has been observed in the Fe $3d$ PES of $SrFeO_3$ and $I(E_F)$ increases with increasing x in $SrMn_{1-x}Fe_xO_3$. These findings agree with the MIT in $SrMn_{1-x}Fe_xO_3$ with decreasing x. In contrast, $I(E_F)$ in Mn $3d$ PES is negligibly small for all x, implying that Fe $3d$ electrons play an important role in determining the metallic conductivity in $SrMn_{1-x}Fe_xO_3$. The GGA band structure calculations for $SrMnO_3$ and $SrFeO_3$ exhibit the same trend in the peak positions as in the experimental PES/XAS spectra.

ACKNOWLEDGMENTS

This work was supported by the NRF under Contracts No. 2009-0064246 and No. 2009-0079947. PLS is supported by POSTECH and MEST in Korea. Work at NIU was supported by the NSF (Grant No. DMR-0706610).

*Corresponding author; kangjs@catholic.ac.kr

[1] J. B. MacChesney, R. C. Sherwood, and J. F. Potter, J. Chem. Phys. **43**, 1907 (1965).
[2] H. Yamada, M. Kawasaki, and Y. Tokura, Appl. Phys. Lett. **80**, 622 (2002).
[3] P. Adler, A. Lebon, V. Damljanović, C. Ulrich, C. Bernhard, A. V. Boris, A. Maljuk, C. T. Lin, and B. Keimer, Phys. Rev. B **73**, 094451 (2006).
[4] H. Falcón, J. A. Barbero, J. A. Alonso, M. J. Martínez-Lope, and J. L. G. Fierro, Chem. Mater. **14**, 2325 (2002).
[5] S. Kolesnik, B. Dabrowski, J. Mais, D. E. Brown, R. Feng, O. Chmaissem, R. Kruk, and C. W. Kimball, Phys. Rev. B **67**, 144402 (2003).
[6] T. Negas and R. S. Roth, J. Solid State Chem. **1**, 409 (1970).
[7] T. Takeda, Y. Yamaguchi, and H. Watanabe, J. Phys. Soc. Jpn. **33**, 967 (1972).
[8] I. D. Fawcett, G. M. Veith, M. Greenblatt, M. Croft, and I. Nowik, Solid State Sci. **2**, 821 (2000).
[9] A. E. Bocquet, A. Fujimori, T. Mizokawa, T. Saitoh, H. Namatame, S. Suga, N. Kimizuka, Y. Takeda, and M. Takano, Phys. Rev. B **45**, 1561 (1992).
[10] J. Matsuno, T. Mizokawa, A. Fujimori, Y. Takeda, S. Kawasaki, and M. Takano, Phys. Rev. B **66**, 193103 (2002).
[11] T. Akao, Y. Azuma, M. Usuda, Y. Nishihata, J. Mizuki, N. Hamada, N. Hayashi, T. Terashima, and M. Takano, Phys. Rev. Lett. **91**, 156405 (2003).
[12] J.-S. Kang, H. J. Lee, G. Kim, D. H. Kim, B. Dabrowski, S. Kolesnik, Hangil Lee, J.-Y. Kim, and B. I, Min, Phys. Rev. B **78**, 054434 (2008).
[13] J.-S. Kang, J. H. Kim, A. Sekiyama, S. Kasai, S. Suga, S. W. Han, K. H. Kim, E. J. Choi, T. Kimura, T. Muro, Y. Saitoh, C. G. Olson, J. H. Shim, and B. I. Min, Phys. Rev. B **68**, 012410 (2003).
[14] J.-S. Kang, C. G. Olson, J. H. Jung, S. T. Lee, T. W. Noh, and B. I. Min, Phys. Rev. B **60**, 13257 (1999).
[15] M. Weinert, E. Wimmer, and A. J. Freeman, Phys. Rev. B **26**, 4571 (1982).
[16] J. P. Perdew, K. Burke, and M. Ernzerhof, Phys. Rev. Lett. **77**, 3865 (1996).
[17] In this band calculation, we have assumed the collinear ferromagnetic structure for $SrFeO_3$ since the band calculation for $SrFeO_3$ having the helical spin ordering is very complicated.
[18] In Fig. 5(a), both of the O $1s$ XAS spectra are shifted by the same amount (−527 eV) to account for the O $1s$ binding energy.
[19] J.-S. Kang, J. H. Hong, D. W. Hwang, J. I. Jeong, S. D. Choi, C. J. Yang, Y. P. Lee, C. G. Olson, K. C. Kang, and B. I. Min, Phys. Rev. B **49**, 16248 (1994).
[20] J. H. Park, S. K. Kwon, and B. I. Min, J. Magn. **12**, 64 (2007).